Dispersion strengthening particles in vanadium microalloyed steels processed by simulated thin slab casting and direct charging. Part 1- processing parameters, mechanical properties and microstructure

Y. Li[*+], J.A. Wilson[†], A.J. Craven[†], P.S. Mitchell[+], D. N. Crowther [o] and T.N. Baker[*]

[*] Metallurgy and Materials Engineering Group, Department of Mechanical Engineering, University of Strathclyde, Glasgow G1 1XJ, Scotland, UK.

+ Vanitec, Winterton House, High Street, Westerham, Kent TN16 1AQ. UK

[†] Department of Physics and Astronomy, University of Glasgow, Glasgow, G12 8QQ, Scotland, UK.

[o] Corus Group, Swinden Technology Centre, Rotherham, S60 3AR,UK.

Keywords:

High strength low alloy (HSLA) steel, Direct charged thin slab process, Precipitation, Dispersion Strengthening,

,.

Author for correspondence

Professor T.N. Baker, Metallurgy and Materials Engineering Group, Department of Mechanical Engineering, University of Strathclyde, Glasgow G1 1XJ, Scotland, UK.

Abstract

A study simulating thin slab continuous casting followed by direct charging into an equalisation furnace has been undertaken based on six low carbon (0.06wt-%) vanadium microalloyed steels. Mechanical and impact test data showed properties were similar or better than those obtained from similar microalloyed conventional thick cast as rolled slabs. The dispersion plus dislocation strengthening was estimated to be in the range 80-250MPa.A detailed TEM/EELS analysis of the dispersion sized sub-15nm particles showed that in all the steels, they were essentially nitrides with little crystalline carbon detected. In the Steels V-Nb, V-Ti and V-Nb-Ti, mixed transition metal nitrides were present. Modelling of equilibrium precipitates in these steels, based on a modified version of ChemSage, predicted that only vanadium rich nitrides would precipitate in austenite but that the C/N ratio would increase through the two phase field and in ferrite. The experimental analytical data clearly points to the thin slab direct charging process, which has substantially higher cooling rates than conventional casting, nucleating non-equilibrium particles in ferrite which are close to stoichiometric nitrides. These did not coarsen during the final stages of processing, but retained their highly stable average size of ~7nm resulting in substantial dispersion strengthening. The results are considered in conjunction with pertinent published literature.

Introduction

The dispersion strengthening contribution (σ_p) to the yield strength (σ_y) in high strength low alloy (HSLA) steels by carbide, nitride and/or carbonitride particles has been discussed for over 40 years. Most of the interest has been in steels containing niobium and/or vanadium additions. Values of σ_p have been calculated based on the Ashby-Orowan equation[1, 2] which assumes that the particles are incoherent and randomly dispersed. The particles size (r) and volume fraction (f) are the main variables which are influenced by the chemical composition of the steel and the processing parameters. Normally, particle stoichiometry has also been assumed. Gladman et al [3, 4] found a satisfactory agreement between the values of σ_p estimated using the Ashby-Orowan approach [1, 2], substituting their experimental data for r and f [3], and the indirect approach based on the Hall-Petch relationship [5, 6]. Usually, dislocation strengthening, σ_d, was either ignored or considered to be low and was assumed to be included in σ_p. For example, in 0.1 wt. %C steels, with typical levels of 0.15 wt.% V or 0.04 wt.% Nb, with an average r of 5nm, σ_p was estimated to be ~100-150MPa. These figures are within the range expected for HSLA steels, continuously cast to 200-250 mm thick slabs and controlled rolled to ~5mm strip [7]. More recently, attention has focussed on thin slab (30-80mm) direct charged (TSDC) steels, where higher cooling rates occur, for example, 18°C/s between the finish rolling temperature (FRT), which is normally ~850°C, and the end of water spray cooling, 550-650°C. Thus conditions far from equilibrium exist. Previous publications by the present authors [8, 9] have reported that in TSDC steels, depending on the equalisation and end cool temperatures, combined contributions of dispersion and dislocation strengthening to the yield strength can reach 250MPa. It is therefore of interest to ascertain if the TSDC process route modifies the dispersion

strengthening particle chemical composition, size range or volume fraction, which could lead to higher values of σ_p. Because of the small ferrite grain size developed, an acceptable level of toughness is maintained.

Thin slab continuous casting followed by direct charging into an equalisation furnace has the potential to replace the traditional thick slab casting process for the production of thin sheet HSLA steel. Capital costs and plant size are reduced because fewer rolling stands are required and no space is needed to store cast slabs prior to rolling [10]. The smaller number of rolling stands and the removal of the need to reheat thick slabs from ambient temperature also leads to reduced energy consumption [11]. The ability to change the composition of the melts quickly enables a rapid response to be made to changes in the market demand for different grades of steel, making the plant more competitive. Also, the use of electric arc furnaces enhances the ability to recycle scrap steel and reduces emissions from the plant [12]. Thus, both economically and environmentally, the thin slab direct charged (TSDC) process offers very significant benefits over the conventional process [13]. However, the thermo-mechanical conditions in the direct process are radically different to those in the conventional process. The slab is much thinner and so the cooling rates are much faster, which potentially leads to segregation effects from dendritic solidification [14, 15]. Because the thin slab is directly charged, it no longer undergoes the $\gamma \rightarrow \alpha \rightarrow \gamma$ phase transitions that occur when a conventional thick slab is cooled to ambient temperature and then reheated prior to rolling. This will modify the elemental distributions and may modify any precipitation that occurs prior to rolling [16]. Finally, much less mechanical deformation is required so that there is a possibility that the as-cast structure has a greater effect on the final microstructure than in the conventional process.

Previous papers by the present authors on TSDC microalloyed vanadium steels have considered the effect of chemical composition of the steel and processing conditions on the mechanical properties [8,9,15] . In addition, the microstructural evolution from the as-cast steel to the final product has been investigated [17-20]. This paper, Part 1, is concerned with the effect dispersion strengthening vanadium precipitates have on the mechanical properties and microstructure of TSDC microalloyed vanadium steels. The thermodynamics and kinetics of precipitate formation are also considered in greater detail. In Part 2, details of the electron energy loss spectroscopy (EELS) quantitative chemical analysis of these particles including the light elements, down to a size of 4nm, is presented.

Experimental techniques

The work was undertaken on six related low carbon (~0.06wt), vanadium steels processed using a simulated TSDC process carried out at the Corus Swinden Technology Centre and shown schematically in Fig.1.

All six steels contained ~0.1wt%V. Steel **V** was the base-line steel with ~0.007wt%N. Steel **V-N** had an increased N level of ~0.02wt%. Steel **V-Ti** had ~0.010 wt%Ti and ~0.017wt%N. The three final steels had ~0.01wt%N with Steel **V-Nb** having ~0.03wt%Nb, Steel **V-Nb-Ti** having ~0.03wt%Nb and ~0.007wt%Ti, and Steel **V-Zr** having ~ 0.008wt%Zr.In addition, the steels typically contained the following levels (in wt%) of other elements Si (0.4), Mn (1.5), P (0.015), S (0.005), Cr (0.08), Mo (0.02), Ni (0.07), Al (0.025), B (<0.0005), Cu (0.07), O (0.007).

The steels were melted in air as ~18kg loads and cast into three moulds to produce 50mm thick ingots. The typical cooling rate at the mid thickness position of the

ingots was 3.5°C/s. The ingots were hot stripped from the mould and transferred directly to an equalising furnace set at one of three equalisation temperatures (1050°C, 1100°C or 1200°C) and held for 30-60 minutes prior to rolling. After equalisation, the ingots were rolled on a laboratory reversing mill to 7 mm strips in 5 passes, which gave a total reduction of 86%. A typical rolling schedule is given in Table 1. The usual interpass time was 6s. After the 4th pass, the strip was held for 25-40s until a temperature of approximately 870°C was reached. Finish rolling temperatures varied from 880°C to 850°C and the total rolling times were in the range of 75-90 s. After rolling, the strip was cooled under water sprays to simulate run-out table cooling, the cooling rate being ~18°C/s. The target for the end cool temperature of the strip was in the range 550-650°C but occasionally process difficulties were encountered which took it out of this range. Following cooling, the strips were immediately put into a furnace set at 600°C and slow cooled to simulate coiling with an average cooling rate of 35°C/h from 600°C to 400°C. The rolling schedule [15], Table 1, shows that most of the deformation was introduced at temperatures above 1000°C and that only the final pass was likely to fall within the temperature range which involved strain induced precipitation in austenite, which is known to be important in Nb steels, but less so in V steels. Samples of the steel were taken and water quenched after casting (A), after equalisation (B) and after the fourth rolling pass (C). The fourth sample was taken from the final product (D). Specimens for mechanical and toughness testing were taken from the final product [8,9,15]. Samples were prepared for optical metallography by standard metallographic techniques, and then etched in 2% nital. The ferrite grain size in the final strip was measured using a linear intercept method with an optical microscope attached to an image analyzer. 250 intercepts were counted.

Carbon extraction replicas were produced from the quarter thickness positions of the final 7mm strip of the fully processed steels. Metallographically prepared specimens were etched with 2% nital before evaporating a thin carbon film onto its surface. Following stripping in 5% nital, the films were washed in methanol and distilled water before being deposited onto Cu mesh grids. The replicas were examined by analytical transmission electron microscopy using a Philips EM400T with an EDAX Phoenix energy dispersive x-ray (EDX) system. The experimental details are given elsewhere [17, 18]. 200 small particles (≤ 25nm) extracted onto the carbon replicas were counted for the size distribution of Steel V-N, following processing at 1050/750°C, Table 2. Thin foils were also studied.

Results

Mechanical and Toughness Properties

The mechanical and toughness properties are given in Table 2. The influence of the steel compositions and processing parameters on the yield stress and Charpy data have been considered in detail previously [8,9]. Here the data for $\sigma_{p+}\sigma_d$ are of particular relevance. Using a modified version of the Hall-Petch equation, an estimate of the combined effect of the strengthening conferred by dispersed incoherent particles and by dislocation strengthening, σ_d, can be obtained. Equation 1 shows that by subtracting the ferrite lattice fraction stress and C+N in solution (σ_o), together with the solid solution (σ_s) and grain size strengthening (σ_g) components from the measured lower yield strength (σ_y),values of $\sigma_{p+}\sigma_d$ can be calculated. Equations (2) to (4) gave σ_o, σ_s and σ_g.

$$\sigma_{p+}\sigma_d = \sigma_y - (\sigma_o + \sigma_s + \sigma_g) \qquad (1)$$

$$\sigma_o = 45 \text{ MPa}^{(21)} \quad (2)$$

$$\sigma_s = 84(Si) + 32(Mn)+38(Cu)+43(Ni)^{(22,23)} \quad (3)$$

$$\sigma_g = 18.1\, d^{-\frac{1}{2}}{}^{(24)} \quad (4)$$

The values of ($\sigma_{p+}\sigma_d$) estimated using the method described above for the present steels are given in Table 2 and shown in Fig. 2 as a function of the solubility product, VxN. In this analysis, it was assumed that strengthening from dislocations and texture was low and similar for all the steels examined. Dislocation densities observed in foils in the present work, supported this view. The data in Fig. 2 and Table 2, show that for specimens with comparable equalisation and end cool temperatures, the addition of titanium to vanadium or vanadium-niobium steels results in a decrease in the lower yield strength and dispersion strengthening, but a corresponding improvement in the Charpy toughness. This was because V-Ti nitrides formed at higher temperatures in austenite due to the lower solubility of these compounds than V nitrides [4].

Microstructure

Ferrite grain sizes of a few microns were obtained in the final product. Fig. 3 shows a graph of ferrite grain size plotted against the product of VxN. There is a general trend for the grain size to decrease as the solubility product VxN increases in Steels V and V-N. Some values of the multiple microalloyed steels follow the same trend, while the addition of Nb or Ti, under some processing conditions, lead to a smaller grain size than the median [9].These results suggest that the recrystallization stop temperature in the present TSDC process is low. Cuboidal precipitates, 0-80nm, which nucleated on the austenite grain boundaries, plus cruciforms, up to 150nm in size in Ti containing steels, played an important role in the grain refinement[19].

Fine precipitates, in the size range 4-15nm, were only observed in the final product of each of the steels. An example of an experimentally determined size distribution for small particles is shown in Fig. 4. The largest number appear in the 4-6nm range, but because the histogram is skewed to the right, the average particle size is 6.5 nm. The particles appear to be nucleated homogeneously, Fig. 5, but distributed throughout the matrix, inhomogeneously. Fig. 6 is a dark field micrograph taken from a carbon extraction replica, which shows an area on the left hand side, which appears to be free of particles, whereas the right hand area in the same grain contains a random dispersion.

The details of the method of determining the composition of the particles and the problems which might arise through changes in the particle composition during the analysis, will be considered in Part 2.

Modelling

The particle composition versus temperature was modelled under equilibrium conditions for the target compositions of all steels using the ChemSage thermodynamic software package with a database modified by A. J. Rose of the Corus Swinden Technology Centre, Rotherham [25]. Fe_3C was included in the calculation but AlN formation was suppressed because it was not observed experimentally. The exception to this was Steel V-N where AlN was observed following an equalisation temperature of 1050^{o}C but not at higher equalisation temperatures [9].Examples of the calculated solution temperatures for Steels V-N and V-Nb are shown in Fig. 7 which also indicate that the particles forming at temperatures above the $\gamma \rightarrow \alpha$ transition temperature in Steel V-N are predicted to be stoichiometric nitrides. Fig. 7b shows that the particles forming above the $\gamma \rightarrow \alpha$ transition temperature of Steel V-Nb contain some carbon, with the *C*/*M* ratio increasing from 0.15 to 0.25 as the temperature falls

from the solution temperature to the $\gamma \rightarrow \alpha$ transition temperature. The calculations for Steel V- Nb -Ti give similar results.

Below the $\gamma \rightarrow \alpha$ transition temperature, a sharp rise in the C content, ie the difference between (N+C) / M and N / M in Fig.7, is predicted. With the exception of Steel V-Ti, the particles are all predicted to have C/M of ~0.5 and $(C+N)/M$ of ~0.85 at 600^{o}C, the target end cool temperature i.e. carbon-rich, slightly sub-stoichiometric carbonitrides.

The modelling described above is for equilibrium conditions. However, the particle analysis presented in ‘’part 2’’, clearly shows that they are essentially vanadium nitrides, suggesting a pronounced departure from equilibrium conditions. There have been some attempts to model non-equilibrium conditions. Most are concerned with niobium microalloyed steels and involve strain induced precipitation in austenite and the effect on recrystallization, for example references [26, 27]. Strain induced precipitation was also found to be important in the nucleation kinetics of Ti carbonitride in austenite [28]. Akben et al [29] compared the relative effectiveness of vanadium and niobium in solution on retarding dynamic precipitation in austenite. They interpret their results as indicating the greater effectiveness of Nb compared with V, when both are in solution, in retarding recrystallization. This leads to recrystallization preceding precipitation of VN in V steels whereas recrystallization is more strongly retarded by the Nb in solution [29]. Thus the former would appear to be the situation in the present work. Another approach to microstructural evolution has been described by Bratland et al [30] who modelled diffusion controlled precipitation using a combination of chemical thermodynamics and kinetic theory. However, the thermodynamic model is based on solubility product data dependent on equilibrium conditions.

In an attempt to model a non-equilibrium situation, the present authors have used ChemSage software to estimate the particle volume fraction, knowing the particle composition determined from the EELS data, described in Part 2.This gave the particle analysis for vanadium nitrides close to stoichiometric VN with little C. Modelling of steel compositions was based on Steel V-N, with levels of carbon (a) 0.06wt%,(b) 0.01wt% and (c) 0.001wt%, with the same level of all the other elements given above to examine level of agreement compared to the EELS particle analysis data. The results are collated in Table 3, which shows the predicted volume fractions of VN and VC. Lowering the carbon from 0.06wt %C to 0.01wt %C has a small effect on the volume fractions, but a significant change is predicted when the carbon is reduced to 0.001wt%. The volume fraction, f, of VN, after 1050°C equalisation, increased to become 88% of the total, compared to ~20% at 0.06 wt% C. The results given in Table 3 show that the main outcome of lowering the carbon content in the steel from 0.06% to 0.001%, to approach that given by the EELS analysis of the vanadium particles, is the large decrease in the total volume fraction of particles precipitated in ferrite and as expected, an increase in the ratio of the volume fraction of VN particles to the total volume fraction of vanadium containing particles precipitated in ferrite, with the same changes in carbon content. Irrespective of the carbon content, assuming that all the nitrogen is combined with vanadium, the maximum volume fraction of VN for Steel VN is 1195x 10^{-6}, which includes that nucleated in austenite. The data predicted for the total volume fraction after equalisation at 1200°C for a steel containing 0.001%C is 708 x10^{-6}, which is only ~60% of that theoretically possible. Therefore this approach also has short comings.

Discussion

Dispersion strengthening

The yield strength of TSDC microalloyed steels is primarily comprised of contributions from the ferrite grain size and dispersion strengthening. The small ferrite grain size recorded in this work, Fig. 3 and Table 2, combined with the large dispersion strengthening contribution, Fig. 2 and Table 2, results in yield strength values which can exceed 600MPa, with satisfactory toughness, also shown in Table 2. Dispersion strengthening in steel is dependent on the volume fraction, particle size and inter-particle spacing of fine particles in ferrite. The size and inter-particle spacing of the fine particles are controlled by the nucleation, growth and coarsening rates. The essential parameter governing the variation in nucleation rate is the chemical driving force for precipitation, while that governing growth and coarsening is the diffusion rate. Increasing the vanadium content increases the volume fraction of the fine particles since the high solubility of V(C, N) in austenite allows almost all the vanadium present in the steel to be available for precipitation in ferrite. Furthermore, vanadium has a much higher affinity for N than C. By increasing the nitrogen content in the steel, the predicted nucleation of N rich V(C, N) is enhanced. A consequence of this is a dispersion of a high volume fraction of fine V(C, N) particles, with a small interparticle spacing. Therefore, increasing the V and N content of a steel could lead to a more effective strengthening by precipitation[31]. With the exception of the VN-ZrN system, where the metal atom size ratio is unfavourable for appreciable inter - solubility, all the other binary nitrides give rise to extensive homogeneity ranges [32]. However, with the TSDC route even in the multiple microalloyed steels, the fine particles in ferrite are essentially V-rich nitrides [9, 18, 20]. Hence the volume fraction of fine particles will rely mainly on the amounts of V and N which are available to

precipitate in ferrite. Fig. 4 shows the size range in a distribution of particles of VN responsible for dispersion strengthening. The average size is ~ 7nm.However, it should be noted that the accuracy of the particle measurements, particularly those <5nm, could be ~ ± 50%. The inhomogeneous nature of the distribution of the fine particles shown in Fig. 6 is considered to arise from interdendritic segregation at the as-cast stage, which is retained through the entire process [33]. Similar inhomogeneous distributions of particles have been observed, for example, NbC in both stainless steels[34] and HSLA steels[35], but the inhomogeneity is invariably ignored in most of the microalloy steels literature or considered to be an artifact arising from the specimen preparation.

Equations (1)-(4) allow values of $\sigma_p + \sigma_d$ to be estimated from a method based on the Hall-Petch relationship. However, assuming the precipitates are incoherent, which the size suggests, then σ_p can be calculated from the Ashby-Orowan equation[1], which for iron alloys is given by Gladman[4] as:

$$\sigma_p\,(\mathrm{MPa}) = 10.8\, f^{1/2} /\ d.\ \ln\left(d/\ 6.125 \times 10^{-4} \right) \qquad (5)$$

where f is the volume fraction of particles and d the average particle diameter in microns. Fig. 8 shows the calculated volume fraction of carbonitride particles in ferrite which are considered to produce dispersion strengthening. Taking Steel V-N as an example, Fig. 8 indicates that following an equalizing treatment at 1100°C, f in ferrite is ~13 x 10^{-4}.This figure is obtained by calculating the total volume fraction of particles which could form and subtracting that which, under equilibrium conditions, precipitated in austenite prior to the $\gamma \rightarrow \alpha$ transformation temperature, which is about 760°C.

Taking d as 6.5nm and substituting in (5) for f and d gives σ_p as 141 MPa.

$$[\sigma_p\,(\mathrm{MPa}) = (10.8 \times (0.0013)^{1/2} / 6.5 \times 10^{-3}).\ \ln (6.5 \times 10^{-3} / 6.125 \times 10^{-4})\ ]$$

Thin foil observations confirm that low dislocation densities (ρ) were present in the final product of Steel V-N. This indicates that ρ was $\leq 10^9$ lines.cm^{-2}.

For iron alloys [36],

$$\sigma_d \text{ (MPa)} = 16.2 \times 10^{-4} . \rho^{1/2} \qquad (6)$$

where ρ is the dislocation density in lines.cm^{-2}.

Therefore when ρ is ~ 10^9 lines.cm^{-2}, σ_d = 51 MPa, giving $\sigma_p+\sigma_d$ = 192 MPa.

This value is at the top end of the range of $\sigma_p+\sigma_d$ in Table 2, and should be compared with the indirect calculation of 163 MPa. The dislocation density would need to reach ~10^{10} lines.cm^{-2} before a similar contribution to that from $\boldsymbol{\sigma_p}$ is found.

When ρ is 10^{10} lines.cm^{-2}, σ_d = 162 MPa.

The effect of processing parameters on mechanical properties was considered in earlier papers [8, 9, 15]. Equalisation temperature is important in relation to the solution temperatures which are respectively for Steel V, 1050°C, Steel V-N, 1106°C, Steel V-Ti, 1443°C, Steel V-Nb, 1189°C, Steel V-Nb-Ti, 1389°C and Steel V-Zr, 1655°C [37], 1732°C [38]. Therefore in these steels the lowest equalisation temperature used in the present work, 1050°C, is predicted to leave some vanadium based particles undissolved in austenite in all but Steel V. In the case of Steel V-N, the strongest effect on $\sigma_p+\sigma_d$ would appear to be through the end cool temperature (ECT) as seen in Table 2. For equalisation temperatures below the solution temperature of the nitrides, ie 1050 and 1100°C, it can be seen that $\sigma_p+\sigma_d$ increases with decreasing ECT .With an equalisation temperature of 1050°C, lowering the ECT from 764°C to 602°C almost doubles the $\sigma_p+\sigma_d$ to 200MPa.

Nitride vs Carbonitride

The historical perception for vanadium microalloyed steels undergoing a decomposition to ferrite has been summarized by Siwecki et al [39]. It is often stated that unless the nitrogen level is <0.005%, initially a high nitrogen carbonitride is formed [40-47]. This precipitate was considered to probably nucleate in austenite and was comprised of a nitride rich core with an intermediate carbonitride layer, followed by a carbide outer case. Theoretically, when all the nitrogen is consumed, the remaining vanadium should combine with carbon. Some publications have considered the nitride to nucleate in austenite and the carbide to nucleate in ferrite. In conventional rolled V-Ti or Nb-Ti steels, experimental observations have reported that the complex Ti-V and Nb-Ti particles frequently had a Ti rich nitride core plus hemispherical caps or a carbide coating/shell (V or Nb rich) [48-51].These characteristics were not present in any of the particles studied in the current work. They are normally found in much larger particles than those being considered here.

Siwecki et al [39] in their work, showed by indirect means based on differences in an observed lower contribution to the yield strength, that the core/layers model was not followed in practice. They explained this result by suggesting that either the lower thermodynamic stability of vanadium carbide relative to vanadium nitride is reflected in strongly decelerated precipitation kinetics for the former, or that vanadium carbide coarsens more rapidly, resulting in the observed lower contribution to the yield strength. Further work at the Swedish Institute of Metals, using a ThermoCal software package, modelled the equilibrium solubility of vanadium carbonitride as a function of temperature, for several levels of nitrogen [52]. The model predicted that for a steel with 0.1%C 0.1%V and 0.02%N, the vanadium particles present in austenite at 900°C would be essentially VN containing < 5%C. This compares well

with the data for Steel V-N given in Fig.8a, which has similar levels of V and N, but 0.06wt% C. In the present work, for Steel V-N, it is predicted that the γ→α transformation temperature is about 760°C, and that VN, close to stoichiometry, commences to precipitate once ferrite is formed. In our EELS analysis of Steel V-N, fine vanadium nitride precipitates containing little C were found. The complex vanadium nitride/carbonitride/carbide particles hypothesized by some were not present. As an explanation for our observations, this only leaves decelerated precipitation kinetics of vanadium carbide relative to vanadium nitride, under the conditions of the simulated thin slab casting and direct charging.

A recent paper by Maugis and Gouné [53] has considered the precipitation of vanadium carbonitride in a steel containing 0.19C,0.215V and 0.015N (all wt%).The ratio of the interstitial atoms is C/N=15. This modelling paper again assumed both a vanadium nitride/carbonitride/carbide complex particle and a local equilibrium at the precipitate-matrix interface and considers only precipitation in austenite. The calculations show that for isothermal heat treatment conditions in austenite, 'the precipitates nucleate as almost pure vanadium nitrides. They subsequently grow at the expense of solute nitrogen. When the nitrogen is exhausted, the solute carbon precipitates and progressively transforms the nitrides into carbonitrides.' In addition, they calculated that for an isothermal treatment at 800°C, 'the initial critical radius of nucleation is about 0.3nm, and that after ~ 20s, the composition of the solid solution reaches a value where the nucleation rate is practically zero and nucleation stops'. In the present work, due to the lower carbon content of the steels of ~0.06wt% compared to 0.19 wt% used by Maugis and Gouné [53], the ratio of C/N is significantly lower at ~4, which would be expected to enhance the probability of VN precipitation preceding that of carbonitride formation. Also, the present authors considered that VN

nucleation commences when the first ferrite is formed, around 760°C. The measured cooling rate of 18°C/s from 760°C to the end cool temperature, then defines the time for precipitation, before the water sprays in effect quench the steel. For Steel V-Ti, equalized at 1100°C, which has the lowest end cool temperature given in Table 2, 537°C, the sample took ~13s to reach the end cool temperature. A time of 13s is well within the 20s calculated by Maugis and Gouné for a nucleus of mostly VN to precipitate under isothermal conditions at 800°C [53]. In addition the diffusion rate of vanadium in ferrite, the rate determining factor for the nucleation of VN, is decreasing as the temperature falls from 760°C to the end cool temperature, which will have a significant effect on the particle growth. Using the data collected by Gladman[4], it is estimated that the decrease in the rate of diffusion of vanadium in ferrite between 760°C and 537°C is 1.6 x 10^4 times. Maugis and Gouné [53] also comment on the importance of the decrease in solubility of VC in austenite and ferrite, shown in Fig 2 of their paper. However, they do not comment on the solubility of VN in austenite and ferrite, and neither does Gladman[4], as the data for VN in ferrite is not included in his book. A good collection of VN solubility equations is given by Rose[54] .Table 4 shows the results of calculations for the three different equations available for the solution temperatures of VN in both austenite and ferrite[38, 55-58]. This is plotted in Fig.9.As an example, taking the data for the constants A and B from Equations 1 and 6 in Table 4 as the best fit, for the solubility of VN in austenite and ferrite respectively, it is found that the decrease in solubility of VN in γ and in α at 760°C is ~ 3.4x ie. the ratio of 2.54x 10^{-5} / 7.4 x 10^{-6}, which is significant, but not substantial.

The thermodynamic modelling approach which provides the best agreement with our modelling, as in Fig.7a, for the situation at the transformation temperature and our

experimental data, is that undertaken by Roberts and Sandberg [56] following the work of Woodhead [59]. They[56] considered the separate cases of interphase and random precipitation in ferrite. Both papers concluded that for microalloyed steels, with less than 0.2 wt% C and levels of N up to 0.02wt%, in the case of randomly precipitated particles in austenite or ferrite, they would have a composition close to stoichiometric VN. A regular solution, and equilibrium condition were assumed by both sets of authors[56, 59]. Using the equations derived by Roberts and Sandberg [56] and substituting the chemical composition for Steel V-N, for precipitation in ferrite at 600°C, it is predicted that the particle composition would be V $(C_{0.01}\ N_{0.99})$.

As mentioned above, one of the interesting observations in the present work is the relatively narrow size distribution of VN type particles considered to be associated with a large contribution to the yield strength, through dispersion strengthening [8, 9]. For example, in the final 7mm strip of Steel V-N, following equalizing at 1050°C, Fig. 4, the average particle diameter, d_{ave} was 6.5nm and the distribution showed a single peak, skewed towards the smaller particle sizes. The cut-off was >3x d_{ave}. This strongly suggests that the particles had not coarsened during processing. Due to the high cooling rate of the strip, only ~ 13s elapsed between the final rolling temperature (FRT) and the end cool temperature, Table 1. It is considered that this observation again points to the major fraction of dispersion strengthening particles nucleating during this time. While no detailed work appears to have been undertaken on recrystallization kinetics of as rolled vanadium microalloyed steels, Zajac et al[31] have studied precipitation kinetics during isothermal transformation. Kwon and DeArdo [60] have considered the precipitation and recrystallization kinetics of niobium steels following high temperature compression testing. Testing at 1000°C resulted in a bimodal particle distribution, which the

authors consider to be indicative of particle coarsening, with the smaller particles showing a d_{ave} <12 nm, while the larger had a d_{ave} of ~20nm, which coincided with coarsening. Similar results for niobium steels were reported more recently by Datta et al [27], who concluded that coarsening occurred in both the deformed and undeformed conditions in specimens held at 950°C. Coarsening coincided with particle diameters of ~20nm and ~60nm after holding ~10s and ~100s respectively. All these average particle diameters are significantly larger than the average 6 to 7nm particle size measured in the present work. Furthermore, bimodal distributions of small particles were not observed in the current work. It is suggested that the present TSDC processing conditions involving high cooling rates, resulted in fine scale segregation in the as-cast steel which was retained through to the final product. The high cooling rates following rolling also depress the $\gamma \rightarrow \alpha$ transformation temperature, which is also known to increase the lower yield strength [61]. It is considered that this resulted in the heterogeneous distribution of a high volume fraction of fine incoherent dispersion hardening particles, which in the present work produced a contribution to the yield strength in the range 80-250MPa. The particles were essentially high nitrogen vanadium nitrides, randomly distributed, which because they did not coarsen, are considered to have nucleated in ferrite [31]. Particles of VC were not found in any of the steels. The chemical analysis giving only a VN particle, with no transformation layer from a VN core to a rim of VC, is in contradiction to the model often used to support the hypothesis that VN acts as a nucleus for VC precipitation in ferrite, as suggested again in a recent paper [53].
The present observations fit much better with the ChemSage predictions, Fig. 7, for the particle composition associated with equilibrium precipitation of vanadium nitride

at the $\gamma \rightarrow \alpha$ transformation temperature of ~ 760°C, for a steel of 0.02wt% N and the earlier work of both Roberts and Sandberg[56] and Woodhead [59].

Therefore in our work it is shown that due to the chosen steel compositions combined with the processing conditions used in the laboratory simulation of direct charged thin slab casting, the particle composition close to VNis observed.

Futhermore, in this study, a lack of evidence of either strain induced precipitation in deformed austenite or interphase precipitation, supports the view that the fine random precipitation occurs in ferrite [31].

Conclusions

A study simulating thin slab continuous casting followed by direct charging into an equalisation furnace has been undertaken based on six low carbon (0.06%) vanadium microalloyed steels. It is concluded that;

1 Mechanical and impact test data showed properties were similar or better than those obtained from similar microalloyed conventional thick cast as rolled slabs.

2 The dispersion plus dislocation strengthening was estimated to be in the range 80-250MPa.

3 A detailed TEM/EELS analysis of the dispersion sized particles,4-15nm, showed that in all the steels, they were essentially nitrides with little crystalline carbon detected. In the Steels V-Nb, V-Ti and V-Nb-Ti, mixed transition metal nitrides were present.

4 Modelling of equilibrium precipitates in these steels, based on a modified version of ChemSage, predicted that only VN would precipitate in austenite but that the C/N ratio would increase through the two phase field and in ferrite.

5 The experimental analytical data clearly points to the thin slab direct charging process, which has substantially higher cooling rates than conventional casting,

nucleating non-equilibrium particles in ferrite which are close to stoichiometric nitrides. These did not coarsen during the final stages of processing, but retained their highly stable average size of ~7nm, resulting in substantial dispersion strengthening.

Acknowledgements

The authors would like to thank the following: EPSRC, for financial support under grants GR/M22888 GR/M22918; Corus Group PLC, for financial support, VANITEC, also for financial support. The many useful discussions and advice given by Dr W.B. Morrison is acknowledged, as is the help given by Professor D. Gorman.

References

1 E. Orowan, Symposium on Internal Stresses in Metals and Alloys, London, Inst.Metals, 1948, 451.

2 M. F. Ashby, Oxide Dispersion Strengthening, Ed. G S, Ansell, T D Cooper, F. V. Lenel, 1958, 143-.205, Warrendale, PA Met Soc AIME,

3 T .Gladman, B. Holmes, I.D. McIvor, Effect of Second Phase Particles on the Mechanical Properties of Steel, London, Iron Steel Institute,1971, 68-78.

4 T .Gladman, The Physical Metallurgy of Microalloyed Steels, London, Inst. Materials, 1997, 52.

5 E. O. Hall, Proc. Phys. Soc. London, 1951, **B64**, 747-753.

6 N. J. Petch, J. Iron Steel Inst.1953, **174**, 25-28.

7 J. D. Grozier, 'Microalloying 75', 241-250, 1977, New York, Union Carbide Corp.

8 Y. Li, D.N. Crowther, P.S. Mitchell and T.N. Baker, ISIJ International 2002, **42**, 636- 644.

9 Y. Li, J.A. Wilson, D.N. Crowther, P.S. Mitchell, A.J. Craven and T.N. Baker. ISIJ International 2004, **44**, 1093-1102.

10 R. Kaspar, N. Zentarat and J. C. Herman, Metal Working, 1994, **65**, 279-283.

11 R. Kaspar and O. Pawelski: in Proceedings of the Int. Conf. METEC Congress, 1994, 390- 404, VDEH, Dusseldorf, Germany.

12 P.J. Lubensky, S.L .Wigman and D.J. Johnson, 'Microalloyed 95', 225-233,1995, Pittsburgh (PA), Iron & Steel Soc.

13 V.Leroy, J.C. Herman, 'Microalloying 95', 1995, 213-223, Pittsburgh (PA), Iron & Steel Soc.

14 M. Korchynsky. Scandinavian Journal of Metallurgy 1999, **28**, 40-45.

15 D.N. Crowther, Y. Li, T.N. Baker, M.J.W. Green and P.S. Mitchell, 'Thermomechanical Processing of Steels', 2000, 527-536, London, IOM.

16 P.H.Li, A.K.Ibraheem and R. Priestner, Mat.Sci Forum 1998, **284-286**,517-524.

17 Y. Li, D.N. Crowther, J.A. Wilson, A.J. Craven and T.N. Baker, IOP Conf Ser 2001,**168**, 183-186.

18 J. A. Wilson, A.J. Craven, Y. Li and T.N. Baker, IOP Conf Ser. 2001,**168**, 187- 190.

19 T. N. Baker, Y. Li, J.A. Wilson, A.J. Craven and D.N. Crowther, Materials Science and Technology 2004, **20**, 720-730.

20 Y. Li and T.N.Baker,Mater. Sci. Forum, 2005, **500-501**, 237-244.

21 A. Cracknell and N. J. Petch: Acta. Metall., 1955, **3**,186-189.

22 F. B. Pickering and T. Gladman: ISI Spec. Rep. 81, 1963, 10-20, Iron Steel Inst., London.

23 W. C. Leslie: Metall. Trans., 1972, **3,** 5-36

24 W. B. Morrison and J. A. Chapman: 'Rosenhain Centenary Conference', 1976, 286-303, The Royal Society, London.

25 A. J. Rose: Rep. SL/PM/R/S2971/17/98/A, British Steel Plc, Swinden Technology Centre,(1998).

26 B.Dutta, E.J.Palmiere and C.M. Sellars, Acta. metall. mater., 1992,,**40,** 653-662.

27 B. Datta, E. J Palmiere and C.M Sellars, Acta mater., 2001, **49**, 785-794.

28 W.J.Liu and J.J.Jonas, Met.Trans.A,1995,**26A** , 1641-1657.

29 M.G.Akben, I.Weiss and J.J.Jonas, Acta mater., 1981,**29**,111-121.

30 D.H.Bratland , Ø Grong, H.Shercliff, O.R.Myhr and S.Tjotta, Acta mater.,1997,**45**, 1-22.

31 S.Zajac, T.Siwecki and M.Korchynsky, 'Low –Carbon Steels for the 90's', Ed R.Asfahani and G.Tither, 1993, 139-149, Warrendale, PA, TMS.

32 H.J.Goldschmidt, Interstitial Alloys,1957, 238,Butterworths,London.

33 K.Douse and T.N.Baker, 'Thermomechanical Processing of Steels', 2000, 573-580, London, IOM.

34 C.Y..Barlow, B.Ralph, B.Silverman and A.R.Jones, J.Mat.Sci, 1979, 4,423-430

35 R.M.Poths, PhD Thesis, University of Sheffield, 2003.

36 T.N.Baker, 'Yield, flow and fracture' Ed. T. N. Baker, 1983, 235-273, Applied Science Publishers, London and New York.

37 D.B.Evans, Trans. Met. Soc. AIME,1965, 233,1620-1624

38 K.Narita, Trans ISIJ, 1975,15, 145-152.

39 T. Siwecki, A .Sandberg, W .Roberts, and R. Lagneborg. 'Themomechanical Processing of Austenite', Ed. A.J. deArdo, G.A. Ratz and P.J. Wray, 163-194, 1982, Warrendale, PA, Met. Soc. AIME.

40 H.A. Vogels, P. Konig and K-H, Piehl, Archiv. Eisenh. 1964, **35**, 339-351.

41 T.N. Baker, J. Iron Steel Inst., 1973, **211**, 502-5105

42 T.N.Baker, Metals Tech. 1974, **1**, 126-131

43 D.C. Houghton, G.C. Weatherly and J.D. Embury, 'Themomechanical Processing of Austenite', ed. A.J. deArdo, G.A. Ratz and P.J. Wray , 267-292, 1982, Warrendale, PA, Met. Soc. TMS- AIME.

44 W. Roberts, 'HSLA Steels, Technology and Applications', ed. M .Korchynsky, 33-65, 1984, Metals Park, OH, ASM.

45 J.Strid and K.E. Easterling, Acta metall, 1985, **33**,2057-2074.

46 F.Sun and W.Cui, 'HSLA Steels, Processing, Properties and Technology',

Ed. G. Tither and S. Zhang, 43-50, 1992, Warrendale (PA), TMS-AIME.

47 T .Gladman, 'HSLA Steels, Processing, Properties and Technology', Ed. G .Tither and S. Zhang, 3-14, 1992, Warrendale, PA, TMS-AIME.

48 T. Siwecki, A .Sandberg, W .Roberts, 'HSLA Steels, Technology and Applications', ed. M .Korchynsky,619-634, 1984, Metals Park, OH, ASM.

49 K. He and T. N. Baker: Mater. Sci. Eng., 1993, **A169,** 53-65.

50 R. L. Bodnar, Y. Shen and V. Furdanowicz: Iron Steelmaker, 1999, **26**, 45.

51 R.M.Poths, R.L.Higginson and E.J.Palmiere, Scripta Mater., 2001, **44,**147- 151.

52 S Zajac, 43rd MWSP Conf Proc., ISS, **29**, 2001,497-508.

53 P. Maugis and M. Gouné, Acta mater. 2005, **53,** 3359-3567**.**

54 A.Rose, British Steel Report, 1979,SL/PM/R/S2971/4/97/A

55 E.T.Turkdogan, Trans ISS, Iron and Steelmaker, 1989, May, 61-75

56 W.Roberts and A.Sandberg, Swedish Institute for Metals Report No IM-1489, Stockholm, 1980.

57 V.Raghavan, Bull. Alloy Phase Diagrams, 1984**, 5,** 194-198.

59 M.G.Frohberg and H.Graf, Stahl und Eisen, 1960, **80,** 359- 364.

59 J.H.Woodhead, Proc.Seminar Vanadium in high strength steel, 3- 10,Chicago, 1979,Vanitec, London

60 O Kwon and A J DeArdo, Acta metall. mater.1991, **39**, 529-538.

61 J.H.Bucher and J.D.Grozier, Met.Eng.Quart ,Amer.Soc.Met.,1965,1-6.

Table Captions

Table 1 A rolling schedule typical of that used in the present work

Table 2 Mechanical properties of the steels.

Table 3 ChemSage predictions of the volume fractions, f x 10^6 , of fine precipitates formed in ferrite at 600°C during cooling, based on Steel VN composition, but with three levels of carbon,0.06wt%,0.01wt% ,0.001wt%, and three equalization temperatures, with AlN active.

Table 4 Calculated solubility parameters A and B for VN in austenite and ferrite equation $\log_{10} K_s = A/T + B$, where K_s is the solubility product [V][N] and T the temperature in degrees K. Equation numbers relate to Fig.9.

Figure Captions

1. Schematic diagram showing the process route used for simulating thin slab direct charging. Samples of the steel were taken and water quenched after casting (A), after equalisation (B), after the fourth rolling pass (C) and from the final product (D).

2 Effect of the solubility product [V][N] on the strength.

3 Relationship between VxN and ferrite grain size.

4 Experimentally determined size distribution for small particles for Steel V-N, equalisation temperature1050°C , end cool temperature750° with an average diameter 6.5nm.

5 Fine precipitates in the size range 4-15nm

6 Dark field micrograph which shows a grain on the left hand side, which appears to be free of particles, whereas the right hand grain contains a random dispersion.

7 (a, b) ChemSage modelling of vanadium precipitates in austenite for Steels V-N and V-Nb.

8 Calculated volume fraction of fine precipitates in ferrite for four steels.

9 Solubility of vanadium nitride in austenite and ferrite .

Pass Number	Mill Setting mm	Deformation Per Pass %	Equalisation Temperature °C		
			1200	1100	1050
			Entry Rolling Temperature °C		
1	40	20	1098	1019	978
2	30	25	1088	1013	978
3	20	33	1075	1007	973
4	12	40	1059	1002	972
5	7	42	859	850	862
Typical Finish Rolling Temperature °C			850	850	850

Table 1 A rolling schedule typical of that used in the present work

Steel	Condition			Tensile Properties					Charpy Toughness	
	Equalisation Temp. (°C)	End Cool Temp (°C)	α Grain Size (μm)	LYS (MPa)	UYS (MPa)	UTS (MPa)	EL (%)	$\sigma_{p+}\sigma_d$ (MPa)	J @ –20°C	13J ITT (°C)
V	1100	603	5.6	493	528	617	24	113	72	-100
	1200	537	Bainite	560	540	671	17	-	23	-45
V-N	1050	602	6.2	557		664	24	200	43	-85
		750	6.2	521	544	641	15	163	36	-80
		764	6	466	484	555	10	106	68	-75
	1100	511	5.7	600	606	703	20	236	20	-45
		720	5.3	527	570	644	24	145	35	-45
	1200	646	7.2	489	492	631	19	149	27	-40
		700	6.8	518	529	642	20	173	37	-60
V-Ti	1050	590	5.7	463	500	579	22	86	68	-120
		609	6	459	482	578	26	87	71	-120
	1100	537	4.8	522	526	609	18	137	43	-90
	1200	643	6.6	461	462	571	27	110	45	-100
V-Nb	1050	693	4.5	574	632	674	23	166	52	-105
	1100	647	5.8	544	580	653	17	166	45	-100
	1200	558	5.5	632	655	740	19	247	39	-95
V-Nb-Ti	1050	678	5.9	487	553	599	24	109	76	-75
	1100	603	4.8	547	609	646	24	147	63	-100
	1200	504	5.2	590	625	695	20	197	43	-90
V-Zr	1050	556	4.2	531	554	631	25	107	54	-80
	1100	592	4.8	524	556	623	24	123	46	-80
	1200	678	6.2	508	516	619	26	140	36	-62
		750	7.8	416	430	543	25	64	59	-70
		642	4.8	552	576	655	22	145	30	-80

Table 2 Mechanical properties of the steels.

0.06wt%C	**VN**	**VC**	**Total V particles**	**VN/Total**
1050°C	249	1029	1278	0.195
1100°C	450	1029	1485	0.303
1200°C	456	1029	1485	0.307
0.01wt%C	**VN**	**VC**	**Total V particles**	**VN/Total**
1050°C	302	754	1056	0.286
1100°C	485	754	1239	0.391
1200°C	511	754	1264	0.404
0.001wt%C	**VN**	**VC**	**Total V particles**	**VN/Total**
1050°C	451	49	510	0.884
1100°C	633	49	682	0.928
1200°C	659	49	708	0.931

Table 3 ChemSage predictions of the volume fractions, f x 10^6 , of fine precipitates formed in ferrite at 600°C during cooling, based on Steel VN composition, but with three levels of carbon,0.06wt%,0.01wt% ,0.001wt%, and three equalization temperatures, with AlN active.

	Austenite				Ferrite		
Eqn	A	B	Reference	Eqn.	A	B	Reference
1	-7700	2.86	55	4	-9720	3.90	55
2	-8700	3.63	38	5	-7061	2.26	57
3	-7840	3.02	56	6	-7830	2.45	58

Table 4 Calculated solubility parameters A and B for VN in austenite and ferrite using equation $\log_{10} K_s = A/T + B$, where K_s is the solubility product [V][N] and T the temperature in degrees K. Equation numbers relate to Fig.9.

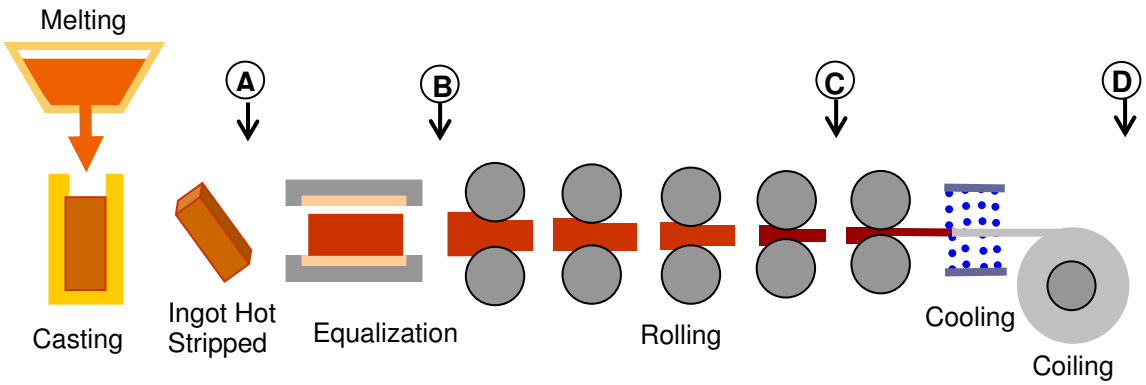

Fig. 1.Schematic diagram showing the process route used for simulating thin slab direct charging.

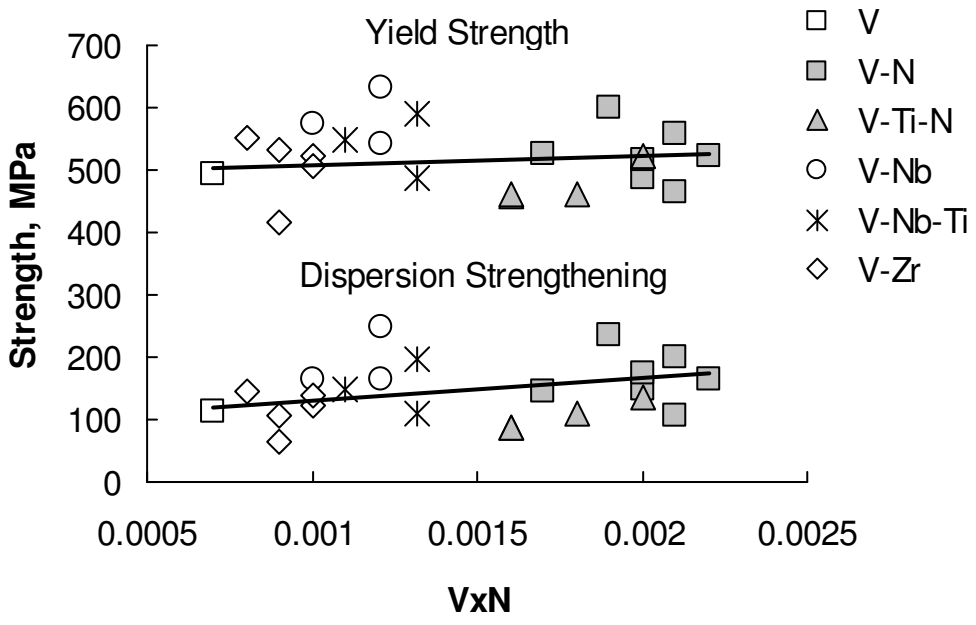

Fig. 2 Effect of the solubility product [V] [N] on the strength.

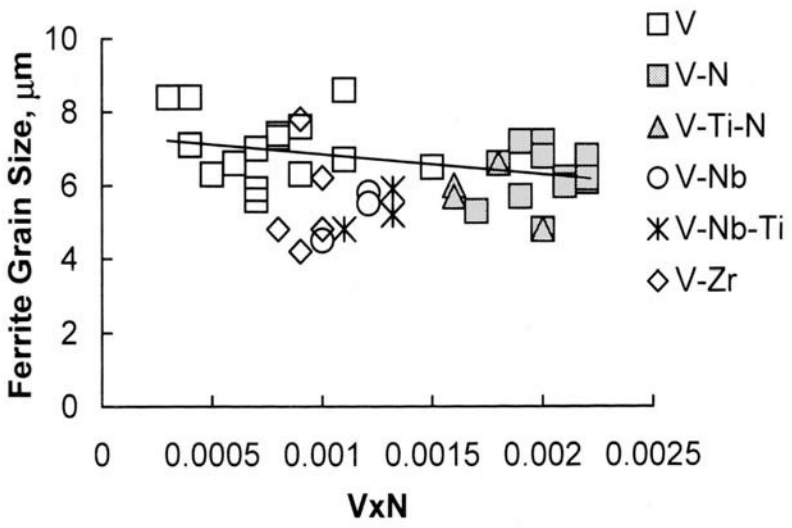

Fig3 Relationship between VxN and ferrite grain size.

,

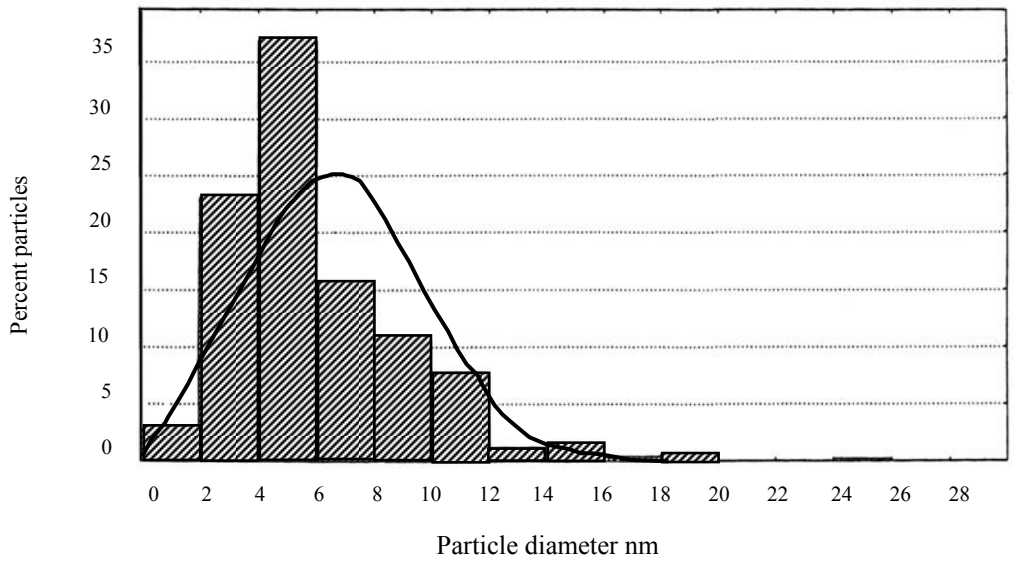

Fig 4 Experimentally determined size distribution for small particles for Steel V-N, equalisation temperature1050°C and end cool temperature 750°, with an average particle diameter of 6.5nm.

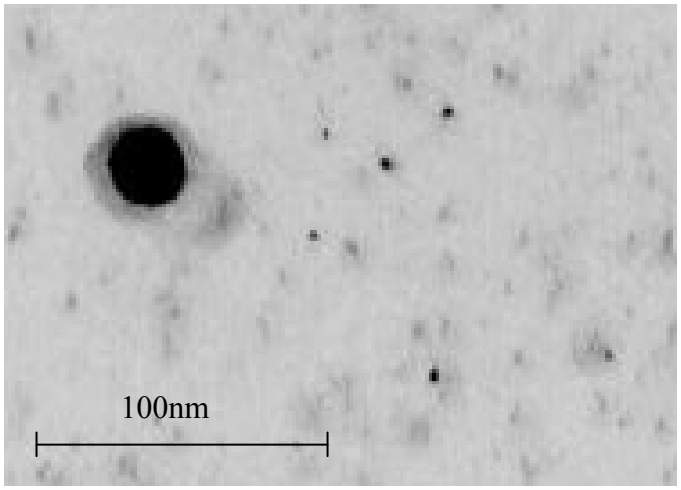

Fig 5 Small precipitates in the size range 4-15nm

with one larger cuboid particle

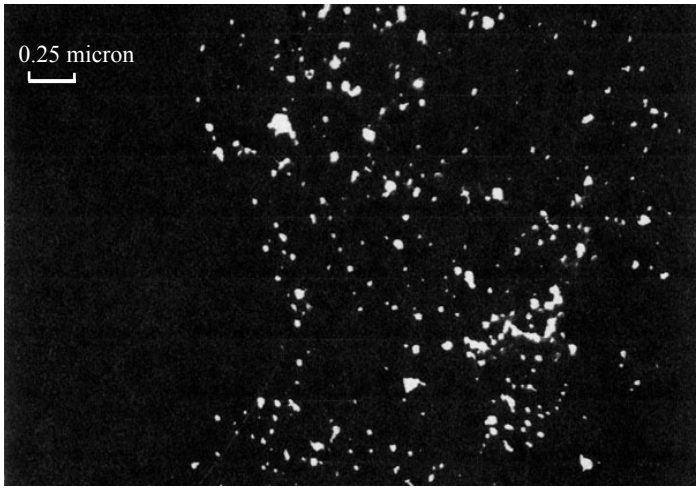

Fig 6 Dark field micrograph which shows a grain on the left hand side, which appears to be free of particles, whereas the right hand grain contains a random dispersion.

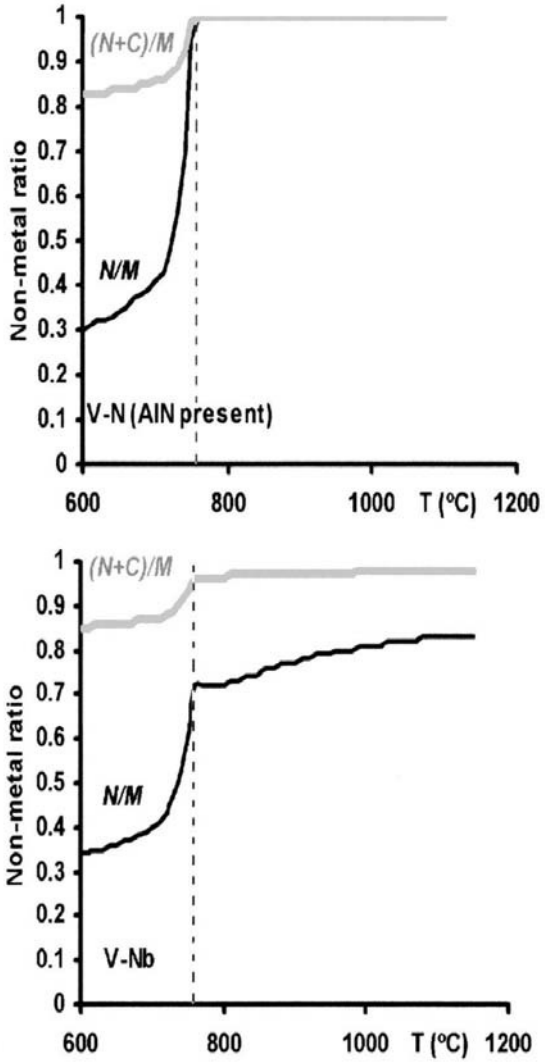

Fig.7 ChemSage modelling of vanadium precipitates in austenite

for Steels V-N and V-Nb

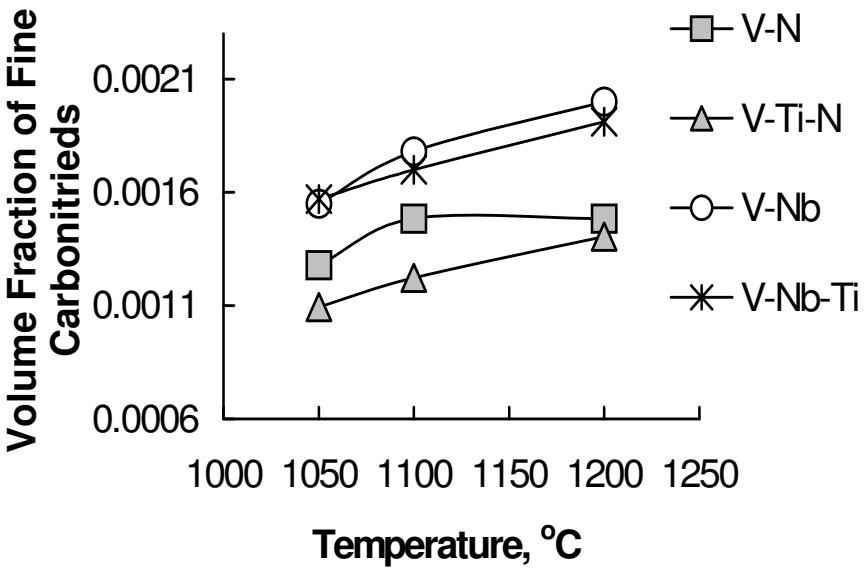

Fig. 8 Calculated volume fraction of fine precipitates in ferrite for four steels

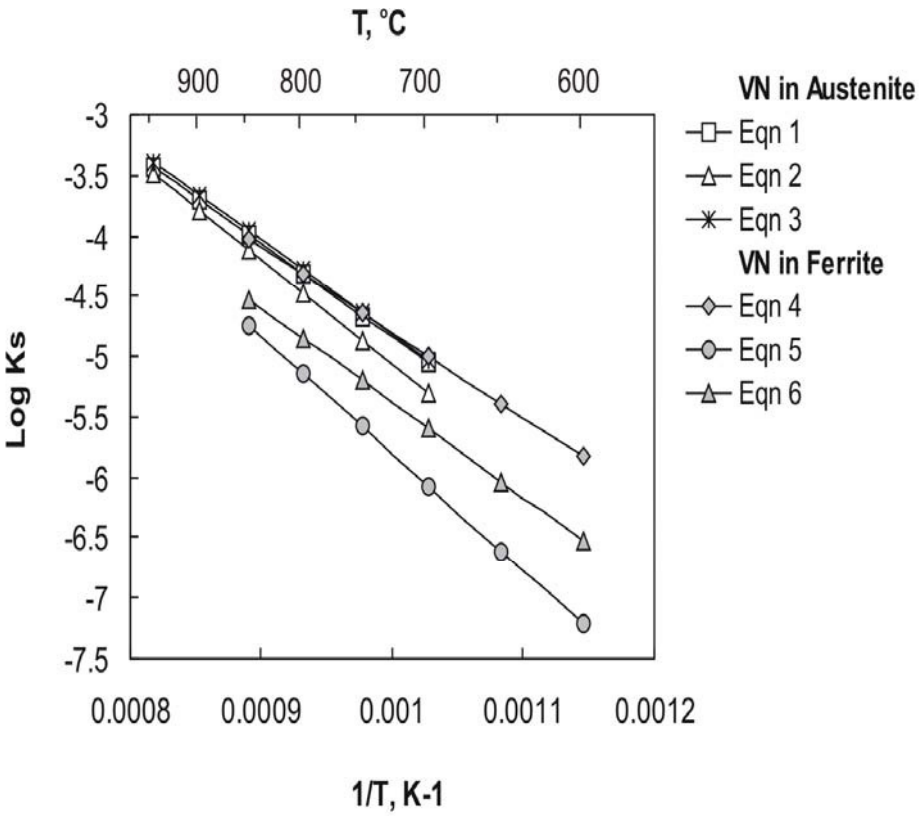

Fig 9 Solubility of vanadium nitride in austenite and ferrite